Atmos. Meas. Tech., 6, 2879–2891, 2013
www.atmos-meas-tech.net/6/2879/2013/
doi:10.5194/amt-6-2879-2013

Atmospheric Measurement Techniques
Open Access

A model-based approach to adjust microwave observations for operational applications: results of a campaign at Munich Airport in winter 2011/2012

J. Güldner

Meteorologisches Observatorium Lindenberg, Richard-Aßmann-Observatorium, Deutscher Wetterdienst,
Am Observatorium 12, 15848 Tauche – OT Lindenberg, Germany

Correspondence to: J. Güldner (juergen.gueldner@dwd.de)

Received: 1 March 2013 – Published in Atmos. Meas. Tech. Discuss.: 22 March 2013
Revised: 20 September 2013 – Accepted: 25 September 2013 – Published: 29 October 2013

Abstract. In the frame of the project "LuFo iPort VIS" which focuses on the implementation of a site-specific visibility forecast, a field campaign was organised to offer detailed information to a numerical fog model. As part of additional observing activities, a 22-channel microwave radiometer profiler (MWRP) was operating at the Munich Airport site in Germany from October 2011 to February 2012 in order to provide vertical temperature and humidity profiles as well as cloud liquid water information. Independently from the model-related aims of the campaign, the MWRP observations were used to study their capabilities to work in operational meteorological networks. Over the past decade a growing quantity of MWRP has been introduced and a user community (MWRnet) was established to encourage activities directed at the set up of an operational network. On that account, the comparability of observations from different network sites plays a fundamental role for any applications in climatology and numerical weather forecast.

In practice, however, systematic temperature and humidity differences (bias) between MWRP retrievals and co-located radiosonde profiles were observed and reported by several authors. This bias can be caused by instrumental offsets and by the absorption model used in the retrieval algorithms as well as by applying a non-representative training data set. At the Lindenberg observatory, besides a neural network provided by the manufacturer, a measurement-based regression method was developed to reduce the bias. These regression operators are calculated on the basis of coincident radiosonde observations and MWRP brightness temperature (TB) measurements. However, MWRP applications in a network require comparable results at just any site, even if no radiosondes are available.

The motivation of this work is directed to a verification of the suitability of the operational local forecast model COSMO-EU of the Deutscher Wetterdienst (DWD) for the calculation of model-based regression operators in order to provide unbiased vertical profiles during the campaign at Munich Airport. The results of this algorithm and the retrievals of a neural network, specially developed for the site, are compared with radiosondes from Oberschleißheim located about 10 km apart from the MWRP site. Outstanding deviations for the lowest levels between 50 and 100 m are discussed. Analogously to the airport experiment, a model-based regression operator was calculated for Lindenberg and compared with both radiosondes and operational results of observation-based methods.

The bias of the retrievals could be considerably reduced and the accuracy, which has been assessed for the airport site, is quite similar to those of the operational radiometer site at Lindenberg above 1 km height. Additional investigations are made to determine the length of the training period necessary for generating best estimates. Thereby three months have proven to be adequate. The results of the study show that on the basis of numerical weather prediction (NWP) model data, available everywhere at any time, the model-based regression method is capable of providing comparable results at a multitude of sites. Furthermore, the approach offers auspicious conditions for automation and continuous updating.

Published by Copernicus Publications on behalf of the European Geosciences Union.

1 Introduction

The campaign of the project LuFo iPort (innovative airport) was organised from October 2011 to February 2012 and had its focus on forecast techniques of poor visibility, one among various weather-related phenomena affecting airport management and traffic. DWD in cooperation with the University of Bonn was implementing a site-specific fog forecasting system for Munich International Airport (Rohn et al., 2010). Therefore the fog forecasting model PAFOG (Bott and Trautmann, 2002) was upgraded in order to integrate local observations from instruments installed close to the runways. Among them, a 22-channel microwave radiometer profiler MP-3000A from Radiometrics (Ware et al., 2003) was operating at the airport site during the campaign to provide additional observations. Independently from the visibility forecasting studies, the MWRP observations can be used to investigate the capabilities of microwave radiometers for applications in operational networks. The challenge here was to retrieve temperature and humidity profiles within the expected error range, although no a priori information are used in advance. That's important, first of all to provide best possible data for subsequent applications in the frame of the project and secondly to simulate any potential stand-alone radiometer site.

Microwave radiation emitted by the atmosphere contains information on temperature, water vapour, and cloud liquid water. A comprehensive review on ground-based microwave radiometry is given by Westwater et al. (2005). The microwave technology has reached a formidable level over the past decade and state-of-the-art radiometers are capable of providing continuous observations in unattended mode during all weather conditions. Thus, the prerequisites exist to start activities towards operational networks. For example, a user community MWRnet (http://cetemps.aquila.infn.it/mwrnet) was established to support ambitions of people working with ground-based radiometers. Furthermore, within the European COST action EG-CLIMET (European Ground-Based Observations of Essential Variables for Climate and Operational Meteorology) efforts have been initiated, e.g. to establish "best practice" for making MWRP observations/retrievals and to develop common retrieval algorithms with error analysis. However, good calibrations and accurate knowledge about radiative transfer are fundamental for achieving progress towards network applications. Comparable results at just any site of a network are indispensable for operational use.

2 Motivation

The importance of the observation bias problem has been recognized for many years. In particular, the increased use of satellite data in numerical forecast models have led to the development of methods to remove systematic radiance differences between computed values and observations (Eyre, 1992; Dee, 2005). The assimilation theory assumes the presence of random and zero-mean errors to optimally combine model predictions with observations. While purely random effects can be handled by filtering methods within an assimilation scheme, observation biases can systematically damage the data assimilation scheme (Auligné et al., 2007). In contrast to the bias of specific satellite instruments, which have regionally a similar structure, the biases of data from ground-based observations in a network can differ from site to site. However, here as well, unbiased measurements are assumed for the application of retrieval algorithms developed to derive vertical profiles.

Experiences obtained during a decade of microwave profiling at the Lindenberg observatory indicate that, in practice, systematic differences in observations and retrievals are not unusual and change over time. Both technical modifications of the instruments and revised retrieval procedures over time can result in relevant variations. Furthermore, discrepancies don't only occur along the time-axis but can also be caused by uncertainties in the microwave absorption models. A model-dependent bias was found by Liljegren et al. (2005) for the K-band channels between 22 and 30 GHz applying data from the Atmospheric Radiation Measurement (ARM) program site near Lamont, Oklahoma. Hewison et al. (2006) compared various radiative transfer model calculations and radiometer observations from Payerne, Switzerland, in cloud-free conditions during an experiment in 2003/2004 and stated that differences are partially due to the applied absorption model. Data from the same campaign at Payerne were used by Cimini et al. (2006) for an analysis of TB differences between two independent radiometers, as there were: Radiometrics TP/WVP-3000 and ASMUWARA, built by IAP of University of Bern. The results showed that discrepancies remain for comparable channels although different channel specifications were taken into account. Löhnert and Maier (2012) evaluate reliability and accuracy of atmospheric temperature profiles derived by the MWRP system HATPRO (Rose et al., 2005) operated at Payerne observatory in the time period from 2006 to 2009. They observed significant TB offsets between radiometer measurements and radiative transfer calculations during clear-sky situations. A comparison of retrievals with simultaneous radiosondes revealed systematic differences ranging from -0.6 to $+0.3$ K for the lowest 4 km. The deviations had been considerably reduced to smaller than ± 0.1 K when a TB offset correction was used. Additionally, liquid nitrogen calibration can result in offset changes as reported in the same work. Cadeddu et al. (2013) estimate a temperature bias between microwave retrievals and radiosonde profiles ranging from -1 K to $+1$ K up to 1 km, increasing to -2 K for height levels above 2 km. For the comparison data from October 2012 were analysed, collected at the first ARM mobile facility. For water vapor a maximum mean deviation of 2 g m^{-3} was found at a height of about 1.2 km.

In view of these facts, techniques are needed to compensate the well-known deficiencies. At the Lindenberg observatory an observation-based regression method $\mathrm{REG_{obs}}$ has been developed and successfully applied using MWRP and radiosonde measurements from the past to calculate regression operators. The method removes systematic errors and produces weak-biased retrievals with respect to radiosondes (Güldner and Spänkuch, 2001). The approach enables the observation of the diurnal cycle and their important underlying physical processes. The temperature diurnal variation induced by solar heating as well as the water vapor cycle influenced by precipitation, moist convection and evapotranspiration can be recognized by microwave observation as shown by Güldner and Leps (2005). This technique is quite mature and used operationally.

The need of adjustments in order to provide both comparable results over longer time periods and bias-reduced temperature and humidity profiles for practical application is demonstrated in Fig. 1. Given are bias and standard deviations (STD) of temperature and vapor density from June to August in different years representative for the entire period. Figures of this kind can be generated operationally to evaluate the quality of continuous MWRP observations. Compared are both real-time results of the neural net (NN) which had been used in the considered period (Solheim et al., 1998) and the real-time retrievals derived by the $\mathrm{REG_{obs}}$ operator calculated by TB vs. radiosonde combinations from a past period. For temperature the STD of NN and $\mathrm{REG_{obs}}$ are quite similar, ranging from about 0.5 K near the surface to about 1–1.3 K at 2 km and remaining less than 2 K up to 6 km. In contrast, the systematic deviations of retrievals are different from one another. Whereas the bias for $\mathrm{REG_{obs}}$ is really small for all examples, the NN differences range from 0 K near the surface to −1 K between 4 and 6 km in summer 2000 (Fig. 1a) and start at 1 K in the lower levels to reach about 0 K above 5 km in 2004 shown in Fig. 1b. In summer 2010 (Fig. 1c) the bias indicate values of even approximately −2 K. The lower panels of Fig. 1 show the accuracy for water vapor density retrievals. The STD of NN and $\mathrm{REG_{obs}}$ are rather in accordance. But here too, the retrievals differ considerably in their bias. During the discussed decade from 2000 to 2010, the MWRP participated at field campaigns and was sent back to factory for repair and upgrades. Furthermore, several calibrations were performed. However, each of these actions can cause systematic differences. The examples demonstrate that the $\mathrm{REG_{obs}}$ method is capable of harmonising MWRP retrievals over time and that any kind of correction has to be applied to provide suitable temperature and humidity profiles.

However, regression methods use radiosonde measurements ($\mathrm{REG_{obs}}$), which have their specific error characteristics. A striking example is the strong dry bias of RS92 radiosondes daytime observations induced by solar radiation. Vömel et al. (2007) quantified the average dry bias increasing from 9 % at the surface to about 50 % at an altitude of 15 km applying data of a campaign in Costa Rica in summer 2005. This means that the amount of water vapor in the tropical upper troposphere is underestimated by the Vaisala RS92 up to a factor of 2. Considerable efforts have been made to develop correction methods including an approach that uses the integrated water vapor content (IWV) derived from microwave radiometer measurements to adjust radiosonde humidity profiles at the ARM SGP site in Oklahoma (Cady-Pereira et al., 2008). Currently, in the frame of GRUAN (GCOS Reference Upper Air Network) activities are forced to provide long-term high-quality climate records. For this purpose an agreed correction method is applied to radiosonde data from all GRUAN sites to provide observations with reference quality, including complete estimates of measurement uncertainty (Immler and Sommer, 2011). These profiles could be used in forthcoming studies to validate retrievals. Nevertheless, the solar radiation induced dry bias in the upper troposphere is the most significant inaccuracy of radiosonde data used in our experiment. In general, the vapor density in the upper troposphere is very low, whereas in the lower troposphere the observation error is comparatively small. Looking at the intercomparisons of the humidity retrievals displayed in Fig. 1a, it seems more likely that radiometer or calibration inaccuracies cause a varying humidity bias of the NN retrievals in different years and not the quite constant radiation-induced dry bias.

Figure 2 shows a further proof that the comparability of microwave observations is not trivial and can not be expected necessarily within a radiometer network. Compared are 144 ten-minute mean values of corresponding channels of the Radiometrics TP/WVP 3000 (MWRP1) and MP-3000A (MWRP2). Channels from 1 to 5 are arranged in the K-band from 22.23 to 30 GHz and the remaining seven channels along the oxygen complex between 51.25 and 58.8 GHz. The observations differ most for channel 1 (ch1) and ch5 at frequency 22.35 and 30 GHz, respectively. In the V-band ch6 and ch7 (51.25 and 52.28 GHz) have maximum differences. Thereby MWRP1 measures higher TB values for ch1 and ch5 whereas the opposite is the case for ch6 and ch7. TB differences on different days are quite similar for comparable atmospheric conditions if they are close in time to each other and no calibrations are performed in between. That can be concluded from the operational output of plots as given in Fig. 2 (not shown). A specific view is given in Fig. 2b. The radiance was calculated on the basis of the radiosonde (RS) using a radiative transfer model and displayed together with 10 min mean values of both microwave radiometers. Differences of the channel band passes have not been considered. Note, plotted are values at 11:00 UTC when the radiosonde was launched. It can be seen that in some cases MWRP1 and RS agree well, for example ch5 and ch6. For other cases MWRP2 corresponds better with RS, i.e. ch1, ch4 and ch7. However, no statement can be made whether MWRP1 or MWRP2 operates more accurately with respect to RS. It can be merely noted that for each frequency the difference between two radiometers includes a specific bias.

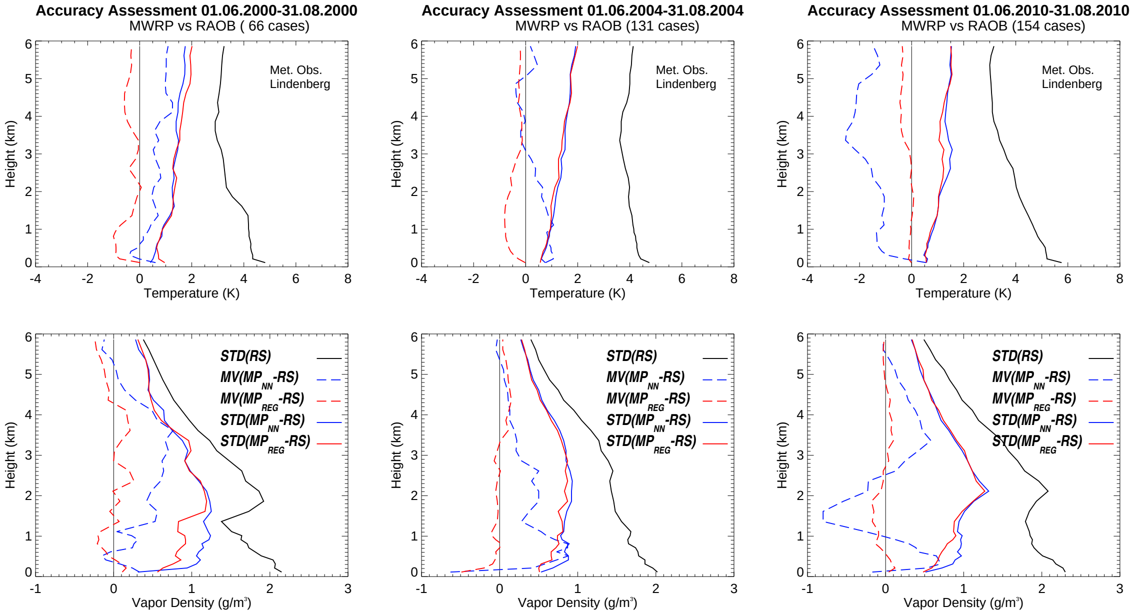

(a) (b) (c)

Fig. 1. Temperature (top) and humidity (bottom) retrieval bias (MV; dashed lines) and standard deviation (STD; solid lines) for different techniques (NN (blue) and $\mathrm{REG_{obs}}$ (red)) calculated for the summer periods 2000 **(a)**, 2004 **(b)**, and 2010 **(c)**. Black lines show STD of radiosondes used in the intercomparison.

We get comparable results if the bias is taken into account as illustrated in Fig. 3. Shown are daily courses of TB differences for the frequencies with minimum and maximum deviations at 30 and 51.2 GHz, respectively. A third curve is plotted for 54.95 GHz which had a mean difference close to zero even from the start. Subsequent to the corrections all deviations matched well.

In conclusion of these facts, it can be stated that corrections of TB observations are necessary if harmonized data are required. This is particularly true for network applications if a multitude of radiometers operate in really unmanned mode. Independent observation-based regression methods have proven their applicability at sophisticated sites equipped with radiosondes. This method compensates radiometer-dependent and radiative transfer model-specific systematic uncertainties.

However, other approaches have also been tested to study the impact of microwave radiometer observations. Variational methods to retrieve profiles of temperature and humidity provide an optimal estimation of combining observations with a forecast model background (Hewison, 2007). The 1-DVAR technique was applied by Cimini et al. (2011) to radiometer measurements during the Vancouver 2010 Winter Olympic Games. Generally was stated that the temperature and humidity retrieval accuracy in the upper troposphere depend primarily on the model analysis, and those in the boundary layer and lower troposphere on the radiometer, respectively. Although the 1-DVAR retrieval skill depends on how well the estimated error-covariance matrices of the background and the observations represent reality, it is expected that the approach avoids inherent retrieval errors to some extent as it benefits from recent data assimilated in the NWP model. The rms errors obtained for 1-DVAR retrievals with and without brightness temperature bias correction, respectively, are quite similar. The comparisons show rms differences within 1.5 K for temperature and 0.5 g $\mathrm{m^{-3}}$ for water vapor density. The retrieval errors are considerably smaller than the observation errors associated to the radiosonde data assimilated in the NWP models. These designated observation errors range from 1.2 to 2 K for temperature and decrease linearly with height from 2.5 g $\mathrm{m^{-3}}$ at the surface to 0.8 g $\mathrm{m^{-3}}$ at 10 km height for humidity. Nevertheless, the presented study is focussed on the harmonisation of microwave observations within a network and on the preparation of data for a subsequent use in NWP models or other applications. This means that measurements at various sites showing different bias characteristics are adjusted to provide site-independent and almost homogeneous error features. The following studies whether an observation-based method can be potentially generalized for applications at various network sites based only on NWP model data.

3 Data sets

The appropriateness of NWP model data to adjust MWRP observations was shown in a study during the LUAMI campaign in November 2008 applying microwave data from

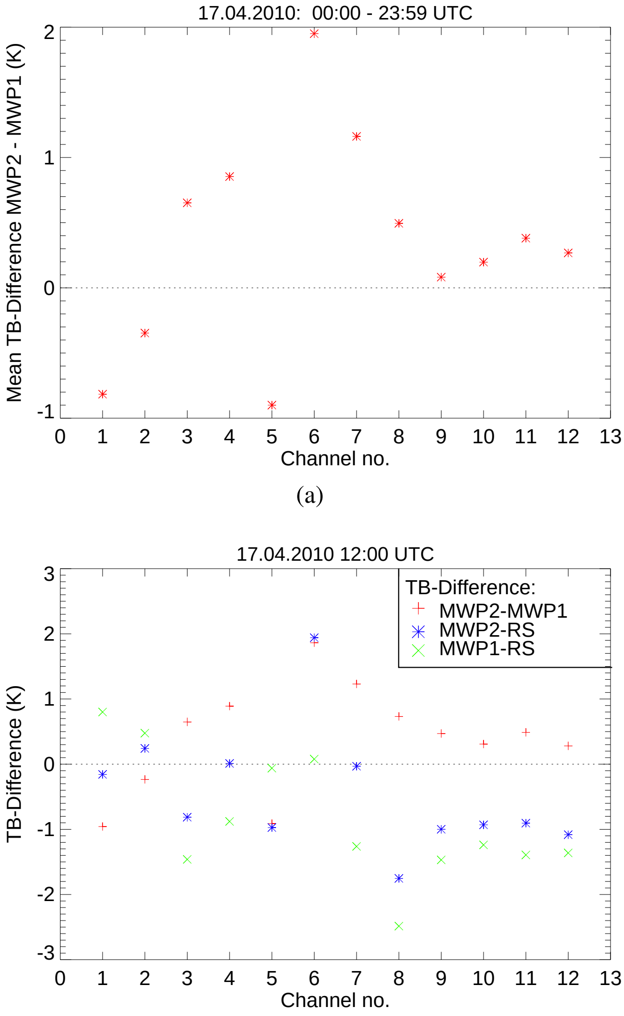

(a)

(b)

Fig. 2. Brightness temperature differences observed by two radiometers operating at the same site. Shown are the mean differences during a cloudless day (17 April 2010) at Lindenberg **(a)** and the deviations from radiative transfer model calculations based on a simultaneous radiosonde **(b)**. The channel numbers correspond to the following frequencies (GHz): 1-(22,24), 2-(23,04), 3-(23,84), 4-(26,24), 5-(30,00), 6-(51,25), 7-(52,28), 8-(53,85), 9-(54,94), 10-(56,66), 11-(57,29), 12-(58,80).

eight stations in Europe (Güldner et al., 2009). In the present work the model-based regression method (REG$_{\mathrm{mod}}$) is analysed in order to get more representative conclusions, made possible through the longer time period of the campaign. In addition, intercomparisons with radiosondes of Oberschleißheim, located approximately 10 km apart, can be performed to assess the accuracy of the REG$_{\mathrm{mod}}$ method. Radiosonde observations are generally only used for validation and not for calculation of REG$_{\mathrm{mod}}$ operators. For the entire period from October 2011 to February 2012, NWP model data for the grid point representing the airport site

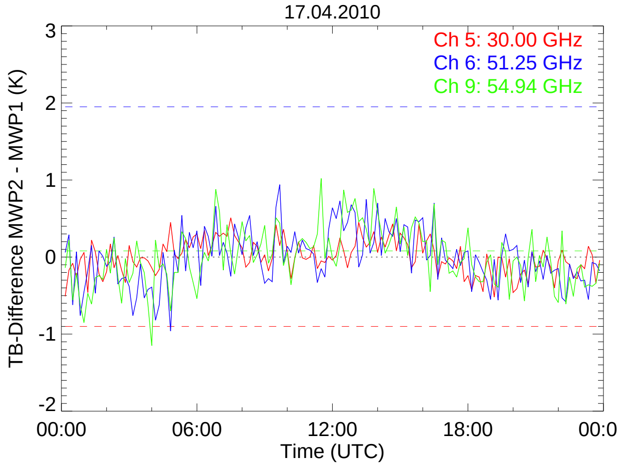

Fig. 3. Bias (dashed lines) and diurnal cycle of unbiased TB deviations from selected channels observed by two microwave radiometers operating at Lindenberg. Shown are data from 17 April 2010 as in Fig. 2.

were extracted from the operational local forecast model (COSMO-EU) of the DWD. The NWP temperature and humidity profiles are available with a temporal resolution of one hour for the model runs started at 00:00 and 12:00 UTC, respectively. In addition, MWRP observations and neural network (NN) retrievals were summed up to 10 min means. However, since only zenith measurements are used in this study, seven to eight measurements are available for each ten minute interval.

In principle, any of the hourly model data sets could be used for the calculation of REG$_{\mathrm{mod}}$ matrices, because for all of these data, TB measurements are available as well. It is recalled that the REG$_{\mathrm{mod}}$ method is based on the combination of coincident forecast profiles and MWRP observations. However, as the NWP model data are strongly correlated if located close together in terms of time, just only one of the hourly data sets of each model run was selected for further application. Generally, the NWP model forecasts at the start time 00:00 and 12:00 UTC, respectively, are representing results of a numerical analysis. These data should be used for REG$_{\mathrm{mod}}$ applications at numerous sites in an operational network because available meteorological information are optimally integrated in the analysis. It should be noted that the presented investigation is directed on the minimisation of systematic deviations at any site of a potential MWRP network and is based on the assumption that the mean profiles of temperature and humidity are homogeneous and weak-biased in respect to the real atmospheric state.

For this study, the complete data set was divided into two groups. One part, containing observations on odd-numbered days was used for training of regression operators. The other independent data set was applied for validation.

4 Results

The $\mathrm{REG}_{\mathrm{mod}}$ or $\mathrm{REG}_{\mathrm{obs}}$ method are specific approaches to the solution of the inverse problem described by the radiative transfer equation (Güldner and Spänkuch, 2001). Estimated profiles $\hat{X}$ are calculated using the equation

$$\hat{X} = x_0 + C_{xy} C_{yy}^{-1} (y - y_0). \qquad (1)$$

C_{xy} represents the covariance matrix of temperature and humidity profiles x, extracted from the NWP model, and the simultaneous MWRP measurements y, which here correspond to TB zenith observations at 22 frequencies, 8 in the K-band ranging from 22.23 to 30 GHz and 14 in the V-band from 51.25 to 58.8 GHz. x_0 and y_0 denote the associated mean values. C_{yy} is the autocovariance matrix of y. Based on this approach various regression operators $\mathrm{REG}_{\mathrm{mod}}$ were calculated.

$\mathrm{REG}_{\mathrm{mod}}$ operators can be calculated as well by including angular information to the zenith observations if horizontal homogeneity is assumed. Crewell and Löhnert (2007) have shown that for temperature a higher accuracy can be achieved by combining angular and spectral information. In this first study only zenith observations are used. In order to generate robust operators for "all-weather" conditions the fine-tuning by using angular observations does not seem to be appropriate, particularly as they are trained with forecast model data. Nevertheless, all prerequisites exist to expand the method by combining with angular observations and should be tested in future experiments.

For a general characterisation of the campaign period, monthly mean profiles of radiosonde observations are calculated and displayed in Fig. 4. Basically, a decrease of temperature and humidity from October to February is apparent. In November 2011, even the mean temperature profile shows a strong inversion. A large number of fog cases was recorded and with regard to the main aim of the campaign, namely a test of site-specific visibility forecasts, it was the most suitable month. Initially, a screening was performed to reject faulty data. Therefore the information of the rain sensor installed on the radiometer was used. Additionally, the brightness temperatures are cross-checked by eye to remove obvious spikes. Appropriate preparations are necessary to avoid inaccurate observations being included in the training data set, which could cause a smearing of interrelations between TB and NWP model data expressed by $\mathrm{REG}_{\mathrm{mod}}$ operators. Moreover, outliers in the validation data set result in incorrect assessments of the retrieval accuracy.

After the screening, and according to Eq. (1), $\mathrm{REG}_{\mathrm{mod}}$ operators are calculated from NWP model data on odd-numbered days at 00:00 and 12:00 UTC, respectively. Matrices are prepared for three different period lengths named as follows:

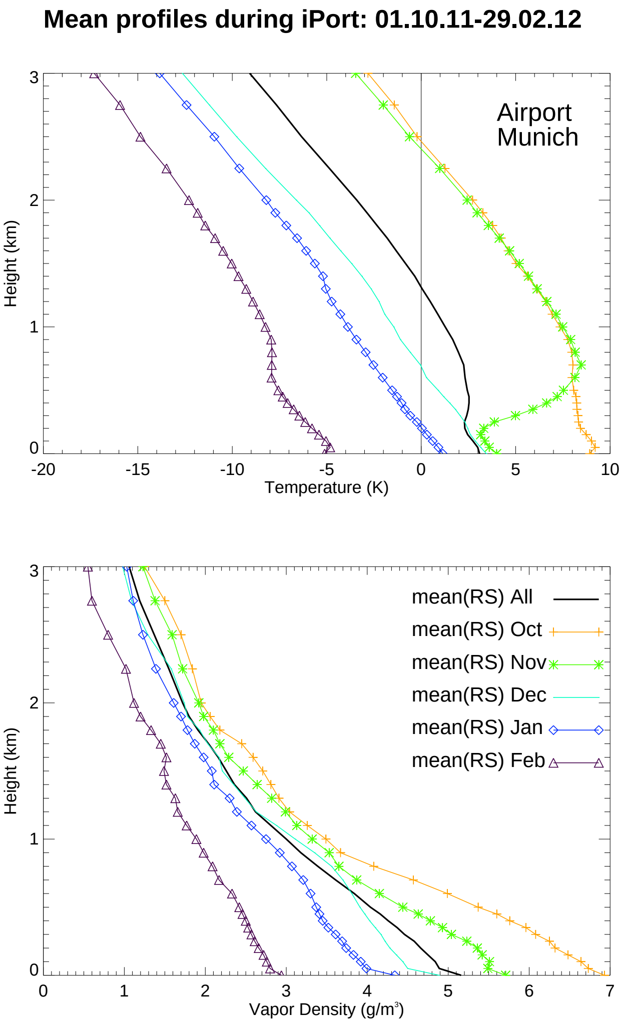

Fig. 4. Monthly mean temperature (top) and vapor density profiles (bottom) during the campaign 2011/2012.

T1mMO: NWP model data of one month (Oct 2011) are used for training (26 cases).

T3mMO: NWP model data of three months (Oct–Dec 2011) are used (72 cases).

T5mMO: NWP model data of five months (Oct 2011–Feb 2012) are used (118 cases).

The even-numbered days of the entire five-month period are generally used as a validation data set. Figure 5 shows the results of this intercomparison calculated on the basis of 104 cases. Plotted are the mean values (MV) of regression retrievals minus radiosonde profiles and the corresponding STD separated according to the different duration of the training periods. Furthermore, the STD of the radiosondes and the results of the NN algorithm provided by the manufacturer are shown. All calculations were done for temperature and vapor density.

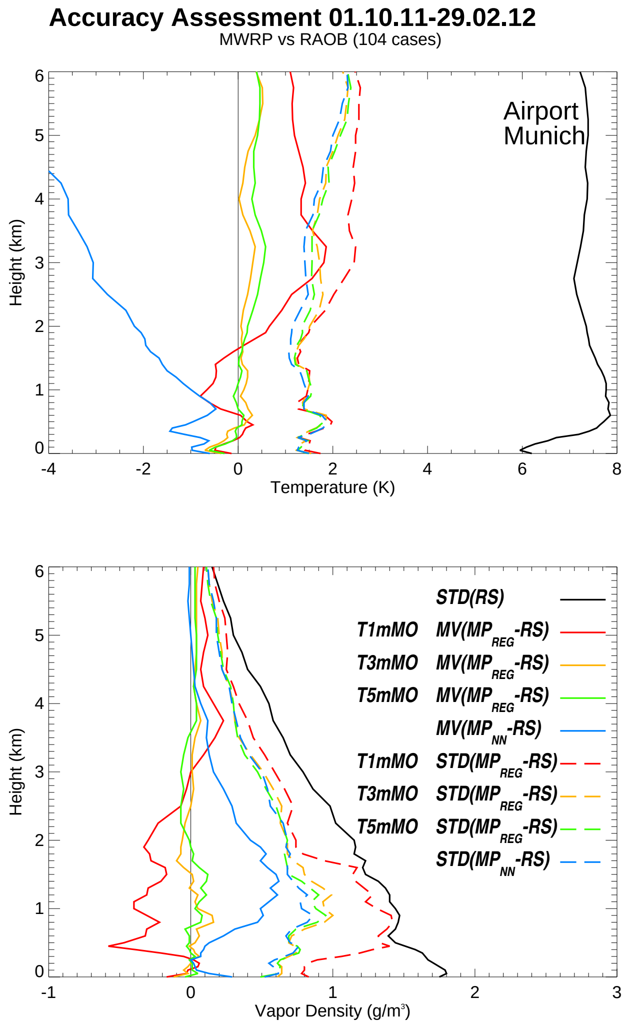

Fig. 5. Retrieval errors of temperature (top) and vapor density (bottom) during the campaign at Munich Airport from October 2011 to February 2012. Plotted are mean values (MV; solid line), defined as retrieval minus radiosonde, and standard deviations (STD; dashed line) for various methods representing different time periods of training. Solid black line shows the STD of radiosondes used in the intercomparison.

The NN retrievals show large negative temperature deviations increasing steadily with height and a significant moist bias above 300 m up to about 4 km. Regarding the regression methods, the largest differences occur if only one month was used for the calculation of $\mathrm{REG}_{\mathrm{mod}}$ operators (T1mMO, red lines). The bias of T1mMO is significantly higher, ranging for temperature from -1 to $+2$ K for heights at 1 km and 3 km, respectively. The STD has greater values above 2 km height for temperature and up to 2 km for water vapor compared to all other retrieval algorithms. Additionally to the small size of the sample used for T1mMO, differences could be induced by the fact that October was the warmest and most humid month of the campaign, and therefore not adequately representative. Consequentially, water vapor retrievals show the largest bias for the T1mMO operator as well. A negative bias was found for levels between 300 m and 2.5 km a.g.l.

In contrast, the results are quite similar if matrices derived from three months (T3mMO, yellow) or five months (T5mMO, green) training periods are applied. It indicates that data of three months may be sufficient for using site-specific $\mathrm{REG}_{\mathrm{mod}}$ operators to reduce systematic errors within a microwave profiler network. The systematic deviations are small and have averaged values limited within 0.5 K for temperature and $0.2\,\mathrm{g\,m^{-3}}$ for vapor density. T3mMO and T5mMO provide temperature retrievals with STD from 1 K to better than 1.5 K, up to approximately 4 km. For humidity, maximum STD of 0.7–$1.0\,\mathrm{g\,m^{-3}}$ are found between 0.5 and 1.5 km. The STD of the $\mathrm{REG}_{\mathrm{mod}}$ humidity profiles is about one half of the radiosonde STD from the surface up to 10 km.

Even though large systematic differences are observed for the NN, the method provides comparable results concerning the STD. For this calculation unbiased retrievals are assumed. Nevertheless, at height levels above 1 km (temperature) and between 0.5 and 1.5 km (humidity) NN provides slightly better retrievals. For water vapor better NN results are achieved exactly for those altitudes, which show a larger STD. The example demonstrates the potential of NN algorithms if systematic deviations could be avoided.

An additional analysis was carried out to demonstrate the "all-weather" capabilities of microwave radiometers. For the training of the $\mathrm{REG}_{\mathrm{mod}}$ operators, pairs of radiometer and NWP model data were used excluding observations disturbed by rain. Cases with precipitation can not be retrieved reliably by the model-based regression method. For the remaining part, retrievals with comparable accuracies are required to make them suitable for network applications and assimilation. In order to examine potential differences the validation data set is divided into two groups, one contains cloudy and the other clear cases. The observations of the infrared pyrometer integrated in the radiometer are used to distinguish between cloudy and clear. The retrievals are assigned to the group of clear cases if the infrared temperatures are less than 230 K and are fairly constant during the 10 min period which was used for the intercomparison. From the total of 104 cases of the validation data set, 38 have been recognized as clear in this way.

The results of the five-month validation data set are shown in Fig. 6. Although the cloud coverage isn't considered for the $\mathrm{REG}_{\mathrm{mod}}$ calculation, the temperature bias for clear cases is lower than the systematic deviation of the cloudy cases above 2 km height. A small advantage becomes apparent for the STD of the clear cases as well. In contrast to that, cloudy retrievals show a smaller bias for lower levels up to 1.5 km. Particularly with regard to the near-surface layers at 50 and 100 m the retrievals have a negative bias compared to RS. That can be caused by deficiencies of NWP models to represent vertical gradients adequately in special weather conditions. Intercomparisons of NWP models showed that the predicted strengths of surface-based inversions were generally to weak compared to the observations (Zhong and Fast, 2003) and that the models underestimate diurnal temperature cycle amplitude at the surface, especially in wintertime nocturnal conditions (Atlaskin and Vihma, 2012). This leads to the question of whether and how inversions are represented by the NWP model in the Munich Airport data set. Figure 7 shows in the top panel mean temperature differences between MWRP, RS and NWP model up to 1 km height, both for all cases and for data estimated as cloudless. For all comparisons, maximum errors of about −0.5 to −1 K were observed between 50 and 100 m a.g.l. In each case the absolute deviation for cloudless conditions was larger than those for all observations. The largest bias was measured between model and radiosondes. In contrast, the difference between REG$_{\mathrm{mod}}$ and NWP model is significantly lower than the deviation between REG$_{\mathrm{mod}}$ and RS indicating that model data are used for the calculation of the retrieval operator.

The bottom panel of Fig. 7 reveals a reason for these unexpected results. Plotted are the temperature deviations between 100 and 0 m of RS profiles on the one hand, and of the model on the other. A total of 212 cases of the whole campaign are displayed. Positive values indicate surface-based temperature inversions and diamonds mark cloudless situations. Obviously, the strong inversions observed by radiosondes are smoothed vertically by the NWP model. Sharp gradients occur mainly under clear sky conditions. The inversions are indeed reproduced, but gradients larger than 2 and up to 8 K are captured as gradients smaller than 2 K by the model. Consequently, the REG$_{\mathrm{mod}}$ method can't retrieve strong inversions if only weak inversions are provided by the training data set. It indicates that specific weather conditions during the campaign and deficiencies of the NWP model to reproduce nocturnal surface-based inversions are mainly responsible for the near-surface bias.

In respect to the water vapor density analysis, a significantly larger bias up to 1.5 km was observed for cloudless conditions as well. In this case too, specific weather situations are responsible for the larger bias in the ground-based layers. Due to the relative low resolution of humidity profiles derived by MWRP measurements, characterised by 2 independent pieces of information (Löhnert and Maier, 2012), strong gradients can't be retrieved satisfactorily. Dry atmospheric air masses characterized by an abrupt decline of humidity are not unusual in wintertime. These situations occur preferably under clear sky conditions. Consequently, retrieval approaches aren't able to reproduce the sharp humidity gradient and the estimated profiles are too moist. This causes a positive bias of clear sky retrievals as given in the bottom panel of Fig. 6. However, we should further take into consideration that water vapor is highly variable in space and time and data from from different sites are compared, located about 10 km from each other. Furthermore, a relatively small number of comparisons are evaluated including 104/38/66 cases for all/clear/cloudy conditions.

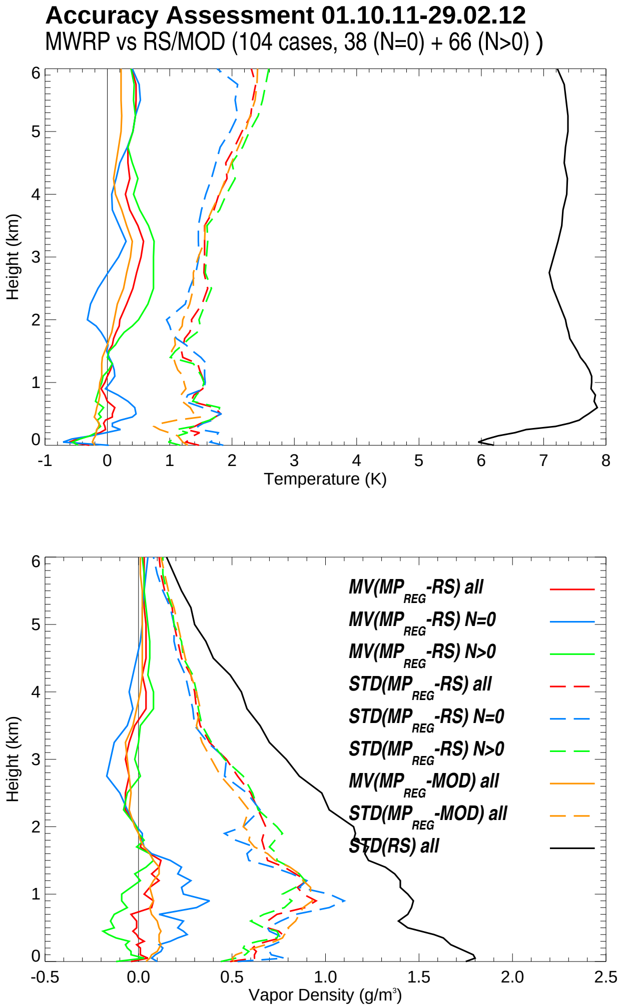

Fig. 6. Retrieval errors of temperature (top panel) and humidity (bottom panel) calculated for Munich (REG$_{\mathrm{mod}}$ was applied). Bias (solid lines) and STD (dashed lines) are plotted for all cases (red), and for cases identified as clear (blue) or cloudy (green). N indicates the cloud cover, where $N = 0$ ($N > 0$) corresponds to cloudless (cloudy) cases.The black lines denote the STD of radiosondes at Munich/Oberschleißheim.

In order to check whether site-specific factors of the airport are responsible for the results, a very similar experiment was performed at Lindenberg observatory simultaneously. A REGmod operator was calculated from a training data set for the period from October 2011 to February 2012. These data include NWP model data (COSMO EU) initialized at 00:00 and 12:00 UTC on odd-numbered days and corresponding MWRP observations. The validation was made by means of radiosondes from 00:00 and 12:00 UTC on even-numbered days. In addition, the operational output both for zenith only REG$_{\mathrm{obs}}$ (Z) and zenith plus 15° elevation observations REG$_{\mathrm{obs}}$ $(Z + E)$ are included in the comparison.

The results are shown in Fig. 8. For temperature the bias of REGmod is generally less than 0.2 K. The STD up to

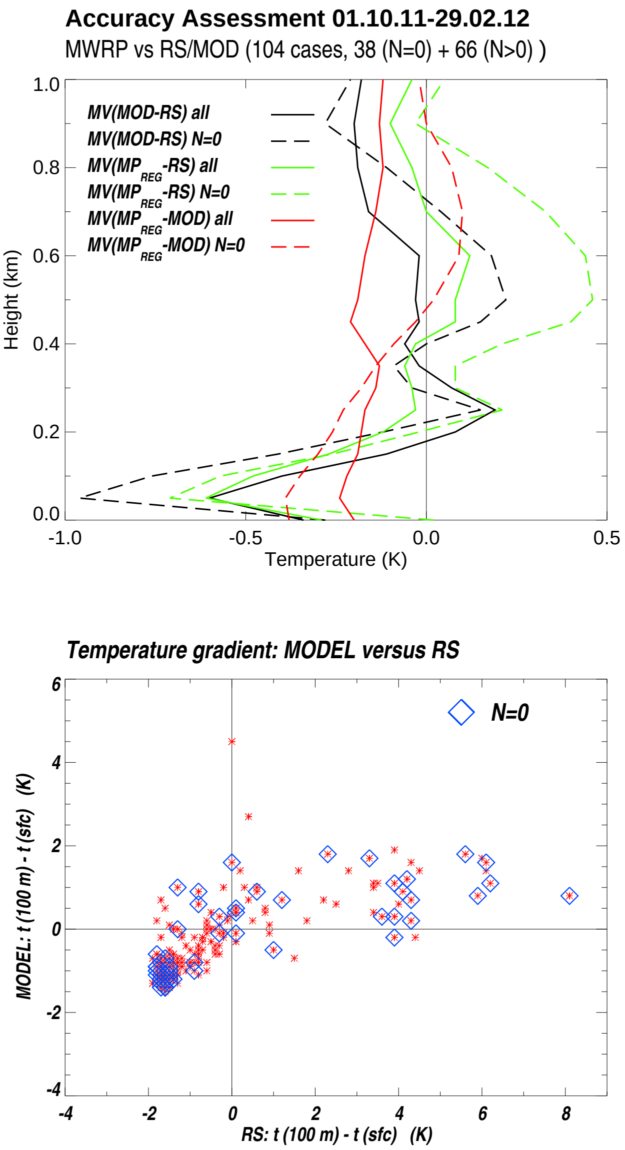

Fig. 7. Mean temperature differences (top panel) between MOD and RS (black), $\mathrm{MP}_{\mathrm{REG}}$ (derived by $\mathrm{REG}_{\mathrm{mod}}$) and RS (green), $\mathrm{MP}_{\mathrm{REG}}$ and MOD (red) for all (solid lines) and cloudless cases (dashed lines). N indicates the cloud cover and $N = 0$ corresponds to cloudless cases. A comparison of temperature gradients of radiosonde (Oberschleißheim) and NWP model data (Munich Airport) for all data (212 cases) in the same period is given in the bottom panel. Cloudless cases are marked by diamonds.

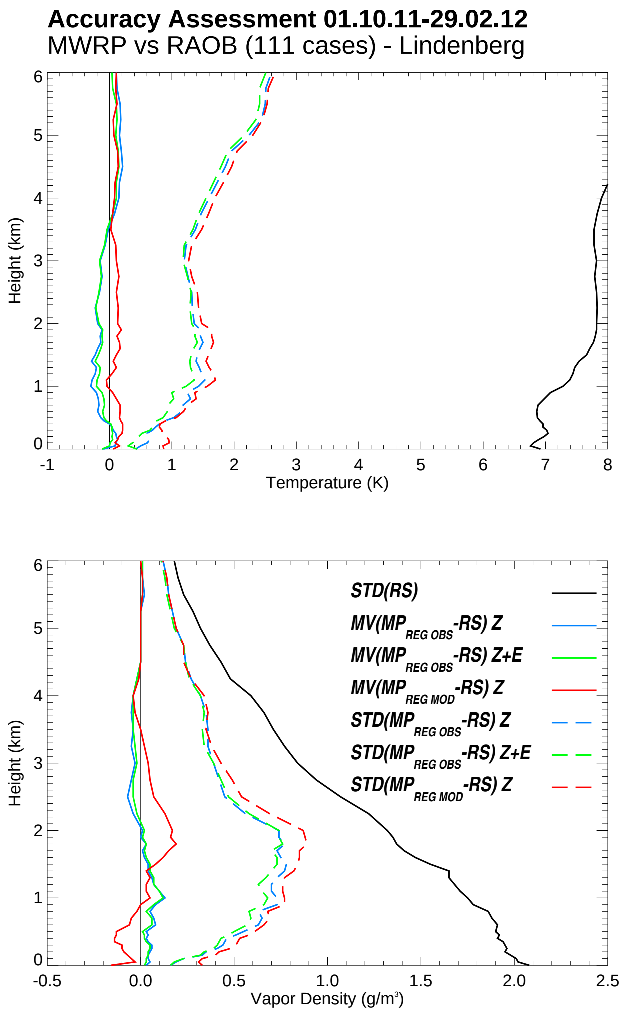

Fig. 8. Retrieval errors of temperature (top panel) and humidity (bottom panel) calculated for Lindenberg. Bias (solid lines) and STD (dashed lines) are plotted for the $\mathrm{REG}_{\mathrm{obs}}$ results if zenith (Z) (blue) and zenith plus elevation ($Z + E$) (green) observations are used as well as for $\mathrm{REG}_{\mathrm{mod}}$ (Z) (red) calculations.The black lines denote the STD of radiosondes.

300 m ranges from 0.8 to 1 K and is about twice as large as the STD of the observation-based $\mathrm{REG}_{\mathrm{obs}}$ methods, whereby $\mathrm{REG}_{\mathrm{obs}}$ ($Z + E$) result in slightly smaller STD. The trend is continuing to a smaller extent between 300 m and 3 km. The results confirm the theoretical expectations that elevation scanning improves the accuracy in the boundary layer. Due to the atmospheric inhomogeneities between the different radiometer fields of view, especially in cloudy conditions, the improvements are limited. Above 3 km, bias are rather in accordance. A similar course is observed for humidity. However, it is notable that up to 3 km both the absolute bias of $\mathrm{REG}_{\mathrm{mod}}$ is larger than the bias of $\mathrm{REG}_{\mathrm{obs}}$ and an evidently smaller STD can be recognized for $\mathrm{REG}_{\mathrm{obs}}$, indicating that additional model errors have an impact on the results of $\mathrm{REG}_{\mathrm{mod}}$ retrievals.

Analogously to Fig. 7, a computation of near-surface differences for Lindenberg was performed and is displayed in Fig. 9. NWP model grid point, launch site of RS and MWRP operation site are very close together in Lindenberg and the strikingly high deviations for the 50 to 100 m levels found at Munich Airport were not present here. In addition to the already discussed limitations of NWP models to capture strong

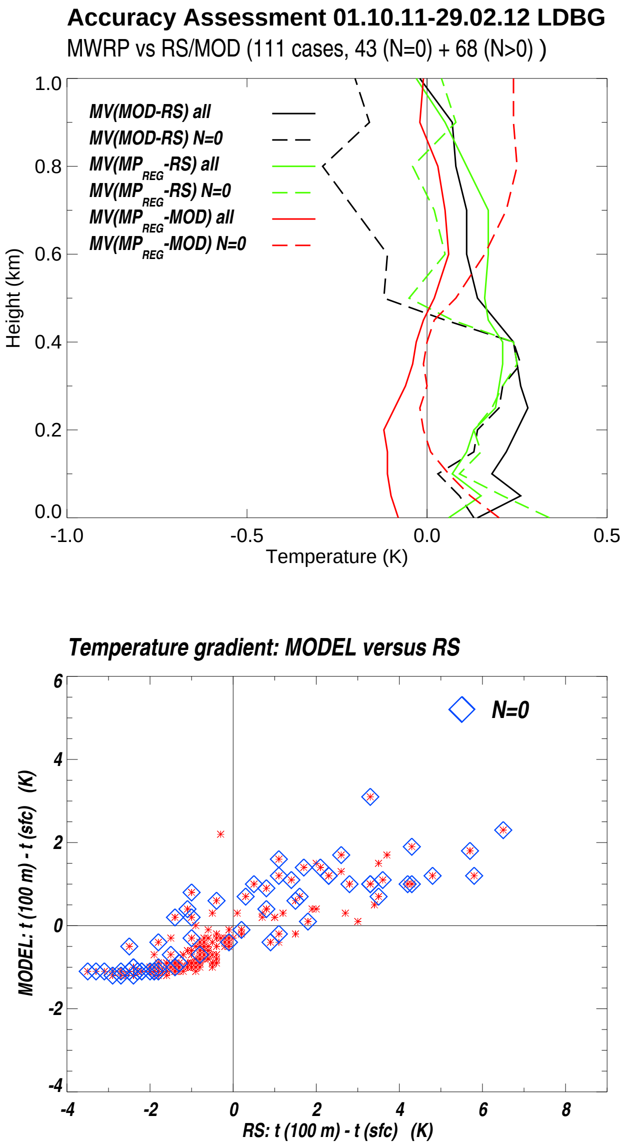

Fig. 9. Mean temperature differences (top panel) between MOD and RS (black), MP_{REG} (derived by REG_{mod}) and RS (green), MP_{REG} and MOD (red) for all (solid lines) and cloudless cases (dashed lines). N indicates the cloud cover and $N = 0$ corresponds to cloudless cases. A comparison of temperature gradients of radiosonde (Lindenberg) and the corresponding NWP model data for all data (240 cases) in the same period is given in the bottom panel. Cloudless cases are marked by diamonds.

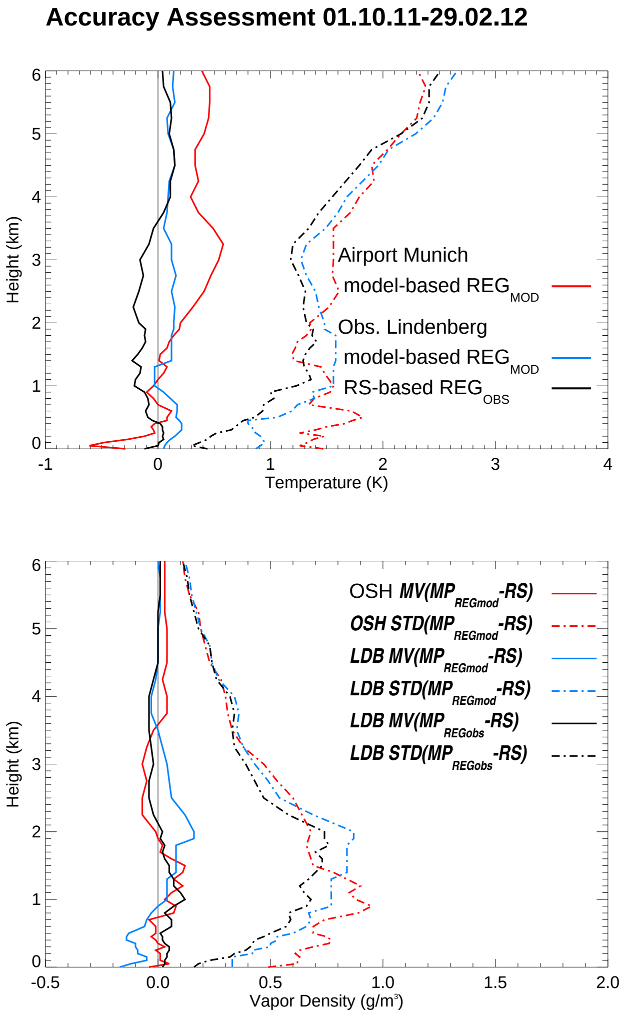

Fig. 10. Bias (MV, solid lines) and STD (dashed lines) of retrieval minus RS deviations for temperature (top) and humidity (bottom) calculated for Lindenberg (REG_{mod} (blue) and REG_{obs} $(Z+E)$ (black) were used) and Munich (REG_{mod} (red) was applied).

gradients, it seems that the RS observations of near-surface levels from Oberschleißheim, which are used for validation, are not representative for the airport grid point of the NWP model. The comparison of the gradients in Lindenberg displayed in the bottom panel of Fig. 9 further shows a smaller spread compared to the analog in Fig. 7 representing Munich Airport, even though the gradients are smoothed here too. By the additional example of Lindenberg it could be shown that REG_{mod} operators generate weak-biased retrievals nearly with the accuracy achieved by the observation-based methods, provided that the NWP grid point is representative of the measurement location.

Finally, a statistic is created, which compares retrievals calculated by the REG_{mod} operator (T5mMO) for the temporary site in Munich with profiles from the reference site at Lindenberg observatory. The airport site is located at 11.48° E longitude, 48.21° N latitude, height 446 m m.s.l. and the Lindenberg site at 14.12° E, 52.21° N, 125 m m.s.l. In Lindenberg temperature and humidity profiles are derived by various retrieval approaches based on radiosonde and in situ MWRP measurements from the past. These REG_{obs} methods have been successfully applied for more than ten years. During the campaign the 12-channel MWRP (TP/WVP 3000) was working in Lindenberg, continuing the

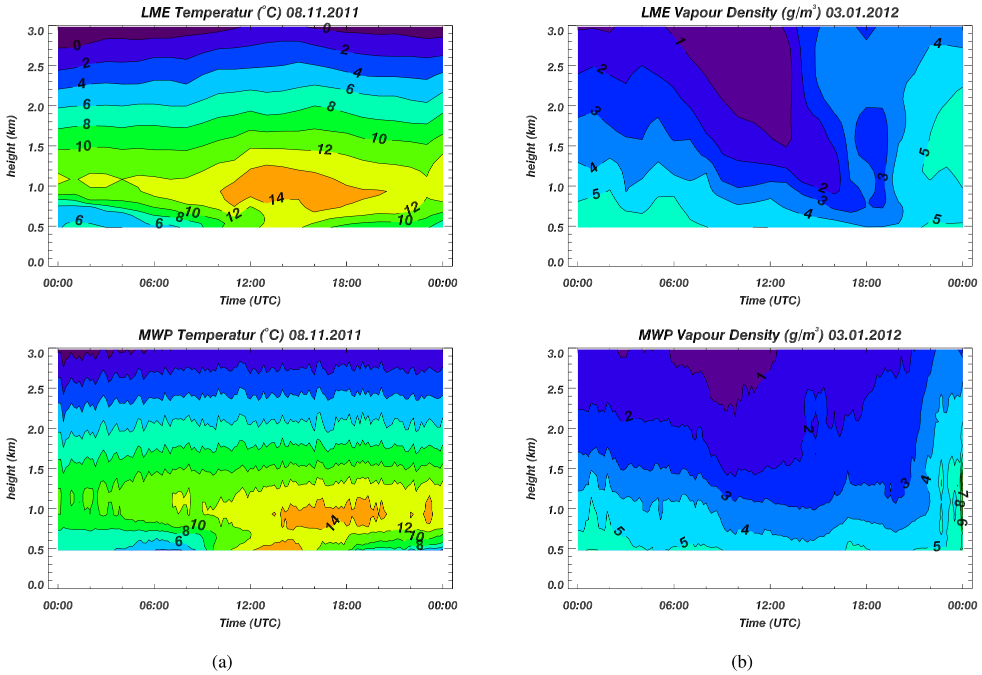

Fig. 11. Comparison of forecast model data (top panels) versus microwave radiometer retrievals (bottom panels) for temperature (left) and water vapor (right).

operational profiling required for the reference site. Provided are retrievals derived from zenith observations and from both zenith and angular observations at an angle of 15° as shown in Fig. 8.

Figure 10 summarizes mean values and STD of Munich and Lindenberg as displayed in Fig. 5 and Fig. 8 calculated with both $\mathrm{REG_{mod}}$ and $\mathrm{REG_{obs}}$ operators. A direct comparison is problematic as the results are influenced by different weather conditions, unequal surface heights and a large distance between the sites. Nevertheless, all methods are solutions of Eq. (1) based on different training data sets and the $\mathrm{REG_{obs}}$ $(Z+E)$ results of Lindenberg can be considered as reference for the potentials and limits of microwave sounding within a profiler network. The absolute temperature bias is less then 0.5 K up to 6 km a.g.l. for all methods. Besides the negative bias close to the surface found for the $\mathrm{REG_{mod}}$ operator, a larger temperature bias above 2 km was also observed in Munich compared to both Lindenberg approaches. The $\mathrm{REG_{mod}}$ STD is smaller as well for Lindenberg up to 800 m and between 2 and 4 km, but is higher in these levels compared to $\mathrm{REG_{obs}}$. For water vapor retrievals the STD shows better accuracies in Lindenberg up to 1.2 km, especially if the $\mathrm{REG_{obs}}$ operator is applied. The bias are rather in accordance for all methods. In general, the temperature and humidity differences of the $\mathrm{REG_{mod}}$ methods have a maximum in the boundary layer caused by the fact that forecast errors are expected to be larger in lower layers. Additionally, it should be taken into account that for the airport site the validation is done with radiosondes launched at a distance of about 10 km. Especially in the lowest layers significant deviations can occur. Both issues can result in additional deviations as found and displayed in Fig. 10.

On an overall basis, the REGmod method provides reasonable results in the expected range. The primary objective of $\mathrm{REG_{mod}}$ is to provide weak-biased retrievals at any site if additional information are not available. $\mathrm{REG_{mod}}$ operators can be updated regularly in order to take into account seasonal variations. However, the operators are least-squares estimates and therefore an optimal compromise of all situations included in the training data set. That defines the limitations of the $\mathrm{REG_{mod}}$ method. Information about the vertical atmospheric structure must be recognisable both in the radiometer observations and the NWP model data. Nevertheless, weak-biased model-consistent temperature and water vapor profiles can be provided continuously.

During the campaign at Munich Airport, the $\mathrm{REG_{mod}}$ algorithm was applied and weak-biased profiles are calculated consistently. Additionally, images of the daily course of temperature and humidity profiles compared with NWP model data are provided as shown in Fig. 11.

5 Conclusions

A MWRP was operating at Munich Airport site from October 2011 to February 2012 to support a campaign aimed at investigations of site-specific visibility forecasts. The radiometer worked reliably and observations were used to simulate procedures required for operational application within a microwave profiler network. In particular, NWP model data were used to produce weak-biased temperature and humidity profiles. In order to provide comparable retrievals, regression operators were calculated on the basis of various training data sets using forecasted profiles and MWRP measurements. Additionally, analog calculations are performed for the Lindenberg observatory. The results of the model-based regression methods $\mathrm{REG_{mod}}$ observed in Munich and Lindenberg and the observation-based regression $\mathrm{REG_{obs}}$ applied at the permanent site Lindenberg were compared. The accuracies of retrievals for both methods are within a similar range above 1 km a.g.l., which was intended to show in the study. The higher differences below 1 km are mainly caused by the use of forecast data instead of in situ observations. Multiple angle information are expected to lead to a reduction of temperature retrieval uncertainty in the boundary layer (Crewell and Löhnert, 2007), though a demonstration for $\mathrm{REG_{mod}}$ is not attempted here.

The usefulness of a model-based regression method to redraw systematic errors and to provide comparable results within a network has been demonstrated, even though limitations became evident, mainly caused by model deficiencies to process specific weather situations. Additionally, the preconditions have been established to make NWP model applications possible. Harmonized brightness temperature values can be provided by forward model calculations of the radiative transfer using the model-consistent algorithm, if required. Furthermore, it is interesting to note that continuous interferences at selected frequencies are recognized by observation-based regression methods. The observations of disturbed channels are automatically devaluated by the site-specific $\mathrm{REG_{mod}}$ operator. Intermittent disturbances can't be detected by the method.

Finally, model data as well as radiometer measurements are always available in operational weather services. That offers good prospects for a continuous and partially autonomous updating of $\mathrm{REG_{mod}}$ operators at a multitude of radiometer sites.

Acknowledgements. This work has been partially embedded in the LuFo/iPort project funded by the Federal Ministry of Economics and Technology (BMWi/LUFO-20V0801C). The author would like to thank to all the staff for the support given for installation and operation of the MWRP at the Munich Airport site. I also thank Angela Christoph (Meteorologisches Observatorium Lindenberg, Richard-Aßmann-Observatorium) for her assistance developing evaluation tools and organising data handling. The author acknowledges the constructive comments of the anonymous referees. Part of this work has been stimulated through the EU COST action ES0702 EG-CLIMET.

Edited by: D. Cimini

References

Atlaskin, E. and Vihma, T.: Evaluation of NWP results for wintertime nocturnal boundary-layer temperatures over Europe and Finland, Q. J. Roy. Meteorol. Soc., 138, 1440–1451, doi:10.1002/qj.1885, 2012.

Auligné, T., McNally, A. P., and Dee, D. P.: Adaptive bias correction for satellite data in a numerical weather prediction system, Q. J. Roy. Meteorol. Soc., 133, 631–642, 2007.

Bott, A. and Trautmann, T.: PAFOG – A new efficient forecast model of radiation fog and low-level stratiform clouds, Atmos. Res., 64, 191–203, 2002.

Cadeddu, M. P., Liljegren, J. C., and Turner, D. D.: The Atmospheric radiation measurement (ARM) program network of microwave radiometers: instrumentation, data, and retrievals, Atmos. Meas. Tech., 6, 2359–2372, doi:10.5194/amt-6-2359-2013, 2013.

Cady-Pereira, K. E., Shephard, M. W., Turner, D. D., Mlawer, E. J., Clough, S. A., and Wagner, T. J.: Improved daytime column-integrated precipitable water vapour from Vaisala radiosonde humidity sensors, J. Atmos. Ocean. Technol., 21, 873–883, doi:10.1175/2007JTECHA1027.1, 2008.

Cimini, D., Hewison, T. J., and Martin, L.: Comparison of brightness temperatures observed from ground-based microwave radiometer during TUC, Meteorol. Z., 15, 19–25, 2006.

Cimini, D., Campos, E., Ware, R., Albers, S., Giuliani, G., Oreamuno, J., Joe, P., Koch, S. E., Cober, S., and Westwater, E.: Thermodynamic Atmospheric Profiling during the 2010 Winter Olympics Using Ground-based Microwave Radiometry, IEEE T. Geosci. Remote, 49, 12, doi:10.1109/TGRS.2011.2154337, 2011.

Crewell, S. and Löhnert, U.: Accuracy of boundary layer temperature profiles retrieved with multifrequency multiangle microwave radiometry, IEEE T. Geosci. Remote, 45, 2195–2201, doi:10.1109/TGRS.2006.888434, 2007.

Dee, D. P.: Bias and data assimilation, Q. J. Roy. Meteorol. Soc., 131, 3323–3343, 2005.

Eyre, J. R.: A bias correction scheme for simulated TOVS brightness temperatures, Technical Memorandum 186, ECMWF, Reading, UK, 1992.

Güldner, J. and Leps, J.-P.: Analysis of CLIWA-NET intensive operation period data as part of the monitoring activities at the German Meteorological Service site Lindenberg, Atmos. Res., 75, 151–166, 2005.

Güldner, J. and Spänkuch, D.: Remote sensing of the thermodynamic state of the atmospheric boundary layer by ground-based microwave radiometry, J. Atmos. Ocean. Technol., 18, 925–933, 2001.

Güldner, J., Christoph, A., Engelbart, D., Ferrario, M. E., Heret, C., Löhnert, U., Madonna, F., Ruffieux, D., Wrench, Ch. L., and Zoll, Y.: Towards the comparability of microwave observations: Results from a temporary profile network during the WMO campaign LUAMI in November 2008, in: Proceedings of the 8th International symposium on Trophospheric Profiling, Delft, The Netherlands, 19–23 October 2009, ISBN 978-90-6960-233-2, 2009.

Hewison, T. J.: 1D-VAR retrieval of temperature and humidity profiles from a ground-based microwave radiometer, IEEE T. Geosci. Remote Sens., 45, 2163–2168, doi:10.1109/TGRS.2007.898091, 2007.

Hewison, T. J., Cimini, D., Martin, L., Gaffard, C., and Nash, J.: Validating clear air absorption model using ground-based microwave radiometers and vice-versa, Meteorol. Z., 15, 27–36, 2006.

Immler, F. J. and Sommer, M.: Brief description of the RS92 GRUAN data produkt (RS92-GDP), GRUAN Tech. Document GRUAN-TD-4, available at: http://www.gruan.org, 2011.

Lilgegren, J. C., Boukabara, S. A., Cady-Pereira, K., and Clough, S. A.: The effect of the half-width of the 22-Ghz water vapor line on retrievals of temperature and water vapor profiles with a twelve - channel microwave radiometer, IEEE T. Geosci. Remote, 43, 1102–1108, 2005.

Löhnert, U. and Maier, O.: Operational profiling of temperature using ground-based microwave radiometry at Payerne: prospects and challenges, Atmos. Meas. Tech., 5, 1121–1134, doi:10.5194/amt-5-1121-2012, 2012.

Rohn, M., Vogel, G., Beckmann, B. R., Röhner, P., Thoma, Ch., Schneider, W., and Bott, A.: iPort-VIS: Site specific fog forecasting for Munich Airport, in: Proceedings of the 5th International Conference on Fog: Fog Collection and Dew, Münster, Germany, 25–30 July 2010, FOGDEW2010-78, 2010.

Rose, T., Crewell, S., Löhnert, U., and Simmer, C.: A network suitable microwave radiometer for operational monitoring of the cloudy atmosphere, Atmos. Res., 75, 183–200, doi:10.1016/j.atmosres.2004.12.005, 2005.

Solheim, F., Godwin, J. R., Westwater, E. R., Han, Y., Keihm, S. J., Marsh, K., and Ware, R.: Radiometric profiling of temperature water vapor and cloud liquid water using various inversion methods, Radio Sci., 33, 393–404, 1998.

Vömel, H., Selkirk, H., Miloshevich, L. M., Valverde-Canossa, J., Valdes, J., Kyrö, E., Kivi, R., Stolz, W., Peng, G., and Diaz, J. A.: Radiation dry bias of the Vaisala RS92 humidity sensor, J. Atmos. Ocean. Technol., 24, 953–963, 2007.

Ware, R., Carpenter, R., Güldner, J., Liljegren, J., Nehrkorn, T., Solheim, F., and Vandenberghe, F.: A multi-channel radiometric profiler of temperature, humidity and cloud liquid, Radio Sci., 38, 8079, doi:10.1029/2002RS002856, 2003.

Westwater, E. R., Crewell, S., Mätzler, C., and Cimini, D.: Principles of surface-based microwave and millimeter wave radiometric remote sensing of the troposphere, Quaderni della Societa Italiana di Elettromagnetismo, 1, 50–90, 2005.

Zhong, S. and Fast, J.: An evaluation of the MM5, RAMS, and Meso-Eta models at subkilometer resolution using VTMX field campaign data in the Salt Lake Valley, Mon. Weather Rev., 131, 1301–1322, 2003.